

Theoretical investigation of F-P cavity mode manipulation by single gold nanoparticles

Xusheng Shi(史旭升), Zhiqiang Luo(罗志强), Zhi-Yuan Li(李志远), and Huakang Yu(虞华康)
Citation: Chin. Phys. B, 2023, 32 (**8**): 084204. DOI: 10.1088/1674-1056/acd2c1
Journal homepage: http://cpb.iphy.ac.cn; http://iopscience.iop.org/cpb

What follows is a list of articles you may be interested in

Dynamic light storage based on controllable electromagnetically induced transparency effect

Liu-Ying Zeng(曾柳莹), Jun-Fang Wu(吴俊芳), and Chao Li(李潮)
Chin. Phys. B, 2023, 32 (**6**): 064213. DOI: 10.1088/1674-1056/acd2bd

Molecular fluorescence significantly enhanced by gold nanoparticles@zeolitic imidazolate framework-8

Yuyi Zhang(张钰伊), Yajie Bian(卞亚杰), Wei Zhang(张炜), Yiting Liu(刘易婷), Xiaolei Zhang(张晓磊),Mengdi Chen(陈梦迪), Bingwen Hu(胡炳文), and Qingyuan Jin(金庆原)
Chin. Phys. B, 2023, 32 (**5**): 054208. DOI: 10.1088/1674-1056/ac81aa

Research progress of low-dimensional metal halide perovskites for lasing applications

Zhen Liu(刘镇), Chun Li(李淳), Qiu-Yu Shang(尚秋宇), Li-Yun Zhao(赵丽云), Yang-Guang Zhong(钟阳光), Yan Gao(高燕), Wen-Na Du(杜文娜), Yang Mi(米阳), Jie Chen(陈杰), Shuai Zhang(张帅), Xin-Feng Liu(刘新风), Ying-Shuang Fu(付英双), Qing Zhang(张青)
Chin. Phys. B, 2018, 27 (**11**): 114209. DOI: 10.1088/1674-1056/27/11/114209

Silicon nanophotonics for on-chip light manipulation

Jingshu Guo(郭敬书), Daoxin Dai(戴道锌)
Chin. Phys. B, 2018, 27 (**10**): 104208. DOI: 10.1088/1674-1056/27/10/104208

Optical manipulation of gold nanoparticles using an optical nanofiber

Li Ying (李英), Hu Yan-Jun (胡艳军)
Chin. Phys. B, 2013, 22 (**3**): 034206. DOI: 10.1088/1674-1056/22/3/034206

RAPID COMMUNICATION

Theoretical investigation of F-P cavity mode manipulation by single gold nanoparticles

Xusheng Shi(史旭升)[†], Zhiqiang Luo(罗志强)[†], Zhi-Yuan Li(李志远), and Huakang Yu(虞华康)[‡]

School of Physics and Optoelectronics, South China University of Technology, Guangzhou 510641, *China*

(Received 9 April 2023; revised manuscript received 3 May 2023; accepted manuscript online 5 May 2023)

The ability to manipulate microlaser is highly desirable towards high-performance optoelectronic devices. Here we demonstrate feasible mode manipulation of Fabry–Pérot type microlasers of a perovskite nanowire via incorporation of single gold nanoparticles. The influences of resonant wavelength, quality factor and emission directions are successively investigated using a two-dimensional finite-difference time-domain method. It is found that blueshift of resonant wavelength could be achieved together with either promoted or degraded quality factor of the microlaser via single Au NPs with varied sizes. Unidirectional emission could also be realized which is favorable for on-chip integration. Our results provide useful reference for feasible manipulation of light–matter interactions and mode selection.

Keywords: microlaser, mode manipulation, gold nanoparticle

PACS: 42.82.–m, 78.67.Bf **DOI:** 10.1088/1674-1056/acd2c1

1. Introduction

In recent decades, microlasers are intensively investigated due to their unique properties and significant potential for innovation in various technological fields. At the micro/nanoscale, they can generate strong and coherent optical signals and offer enormous potential applications in data storage, sensing, on-chip communication, and so on.[1–8] Since the first realization of microlaser in an InGaAs quantum well in the 1980s,[9] a diverse range of microdisk lasers, photonic crystals, and nanowire microlasers made from various semiconductor gain media have been successfully developed along with the development of micro/nano-processing technology.[10–14] Moreover, the emergence of novel laser gain materials, such as perovskites, has expanded the possibilities for developing integrated microlasers with favorable characteristics, including large refractive index, wide bandgap tunability and easy solution processing.[15–19]

Among various microlaser structures, one-dimensional nanowires are excellent candidates for waveguides or Fabry–Pérot (F-P) cavities and have emerged as promising building blocks for a wide range of optoelectronic devices.[13,20] These low-dimensional microcavities utilize the refractive index difference of the medium (e.g., perovskite) to confine light within the cavity and achieve a miniaturized and highly coherent light source.[21] More superior and flexible controllability of the outgoing laser mode is required for practical applications like single-mode output, mode switching, control of laser output direction, etc.[22–28]

In the past decades, surface plasmon polaritons in metal nanostructures have attracted considerable interest in achieving extremely strong optical confinement of laser modes.[29] Present plasmonic laser includes various structures such as metallic-coated lasers, plasmonic nanowire lasers, and metallic-nanoparticle lasers,[30–35] which not only transcend the traditional optical diffraction limit but also possess a certain degree of tunable capability. Among various metallic nanostructures, metal nanoparticles are favored due to their extreme mode confinement capabilities for manipulating laser modes. To date, most microlasers based on metal nanoparticles have been obtained in clusters or arrays of nanoparticles, with the aim of enhancing photoluminescence.[36–39] Mode manipulation of bottle microresonators was enabled by precise deposition of single gold nanoparticles so as to achieve single mode lasing but lacking of expansibility.[40]

In this paper, we propose a method for manipulating the cavity modes of the F-P laser cavity by single metal nanoparticles. Via introducing a gold nanoparticle (Au NP) at the output facet, parameters of the F-P laser cavity (i.e., a one-dimensional perovskite nanowire) could be tailored efficiently. Numerical simulations are performed to investigate the mechanism and influence of various factors (such as resonant wavelength, quality factor, and emission directions) by using a two-dimensional finite-difference time-domain (2D FDTD) method. Our results provide an alternative approach to manipulating the cavity mode of microlasers in a reconfigurable and tunable manner.

[†]These authors contributed equally to this work.

[‡]Corresponding author. E-mail: hkyu@scut.edu.cn

© 2023 Chinese Physical Society and IOP Publishing Ltd

2. Numerical model

Figure 1(a) depicts a three-dimensional schematic diagram of nanowires (perovskite) attached with an Au NP. The microcavity present within the nanowires is considered as the F-P cavity and this model can be simplified as a two-dimensional (2D) structure. Figure 1(b) shows the simulation parameters of the 2D layout, wherein the length and width of the cavity are denoted by L and W, respectively. The refractive index of the perovskite material forming the cavity is set to be 2.5, with the refractive index of the background as 1. The radius of the Au NP is denoted by R.

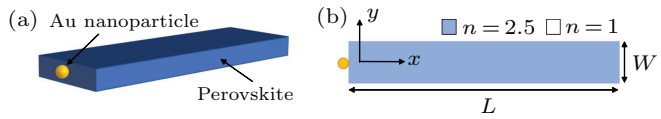


Fig. 1. (a) Three-dimensional schematic of nanowire containing gold nanoparticles. (b) Two-dimensional schematic of nanowire containing gold nanoparticles.

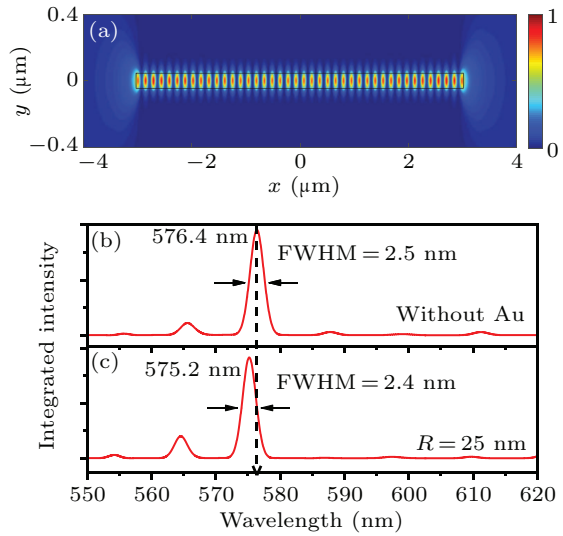


Fig. 2. (a) Field distribution of $|E^2|$ of the nanowire with $L = 6$ μm and $W = 100$ nm. (b)–(c) The simulated spectra before and after the introduction of Au NP, (b) without Au NP, (c) with Au NP (25-nm-radius).

The cavity simulated here is F-P type along the x-axis (as shown in Fig. 1(b)), which is quite common for perovskite microwire lasers. The high refractive index of the perovskite nanowire not only effectively confines photons within the gain medium, but also ensures high reflection from the two end facets, which constitute the optical cavities for light amplification and associated laser output. To maintain the single-mode waveguiding operation, the width of the microwire was set to 100 nm. Figure 2(a) shows a typical field distribution of F-P resonant fundamental mode with a solid black line representing the nanowire. Figure 2(b) displays the integral intensity of the electric field of a rectangular nanowire structure with $L = 6$ μm and $W = 100$ nm. The simulated spectra were obtained through the Fourier transform of the electric fields collected from the monitors that was placed 2 μm away from the end facets. It should be noted that multiple broadband dipole sources (TE-polarized) were used to stimulate resonant modes with random distributions, which gave rise to the non-uniform intensity of resonant modes in our simulation.

3. Results and analysis

Figures 2(b) and 2(c) show the simulated spectra before and after the introduction of single Au NP at the left facet of the perovskite nanowire. The radius of the Au NP is set to be 25 nm. Taking a close look at the main resonance wavelength of 576.4 nm, a clear blueshift is observed due to the attachment of Au NP. For simplicity, the Au NP is placed at the center of the left facet, which would have the most significant impact on the resonant spectra with a blue shift of 1.2 nm.

We also investigate the influence of the nanoparticle size on the resonant spectra. Figures 3(a)–3(e) illustrate the simulated spectra for varied radii of Au NPs. With the increasing nanoparticle radius, the observed blueshift of resonance becomes more obvious and reaches to 1.8 nm for $R = 50$ nm. This result is in accordance with the influencing factor of vertical offset and could be explained by that bigger particle would impinge the reflectance of the light field at the facet to a greater degree. The electric field distributions $|E^2|$ (Figs. 3(f) and 3(g)) show no appearance of high-order modes with increased nanoparticle sizes.

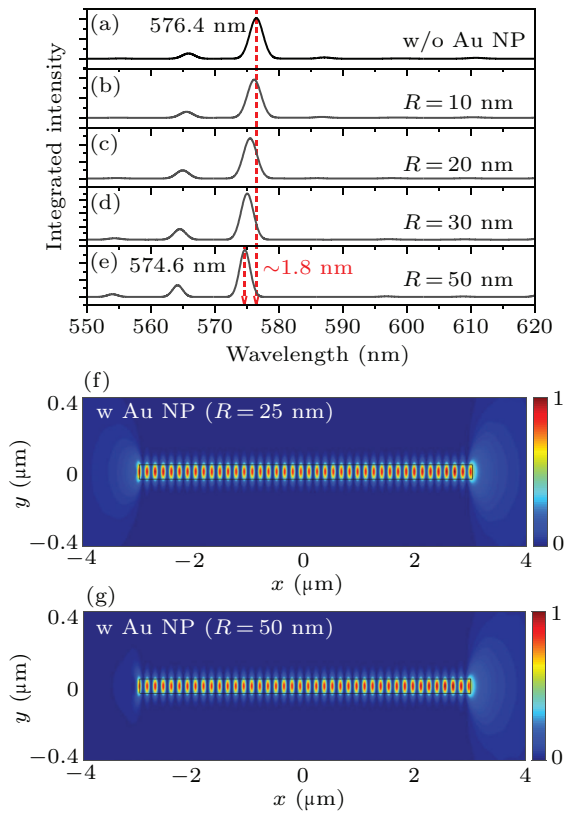


Fig. 3. (a)–(e) Simulated spectra of nanoparticles with different radii. (f) Field distribution $|E^2|$ with Au NP ($R = 25$ nm). (g) Field distribution $|E^2|$ with Au NP ($R = 50$ nm).

It is known that the resonant wavelength should satisfy the resonance formula

$$\frac{2n_{\text{eff}}L}{\lambda} = m \cdot 2\pi + \Delta\varphi_{\text{left}} + \Delta\varphi_{\text{right}}, \tag{1}$$

where n_{eff} represents the effective refractive index of the guided light wave, m denotes the mode number, $\Delta\varphi_{\text{left}}$ and $\Delta\varphi_{\text{right}}$ represent phase shifts on reflection from left and right facets, respectively. According to Figs. 3(f) and 3(g), the mode number is kept unchanged as 42, which is not affected by either introduce of Au NP or change of nanoparticle size. Therefore, one may easily deduce that there is extra phase change $\Delta\varphi'_{\text{left}}$ on the left facet as a result of the attachment of Au NP. The emergence of $\Delta\varphi'_{\text{left}}$ is responsible for the blueshift of resonant wavelength $\Delta\lambda$ according to Eq. (1) for the unchanged mode number.

To study the influence of Au NP, the local field and phase distributions of the main electric field E_z at the resonant wavelength on the left facets are shown in Figs. 4(a)–4(d). The solid black lines represent rectangular microcavity while the black dotted lines represent gold nanoparticle with a radius of 25 nm. By comparing two phase diagrams, we could extract an extra phase difference of approximately 0.73 rad with the attachment of Au NP, corresponding to a calculated wavelength change of 1.28 nm from Eq. (1). This calculated number is in good agreement with blueshift as shown in Figs. 2(b) and 2(c). It is believed that such extra phase retardation originates from the change from dielectric–air (i.e., perovskite–air) interface to dielectric–metal (i.e., perovskite–gold) interface of the end facet. Furthermore, we study the influence of nanoparticle sizes on extra phase differences as shown in Fig. 4(e). It can be found that the additionally introduced phase difference is positively correlated with the radius of nanoparticles. This point is reasonable because as the radius of the nanoparticle increases, the perovskite–gold interface of the end facet becomes larger, and more phase change could be introduced over the entire end facet.

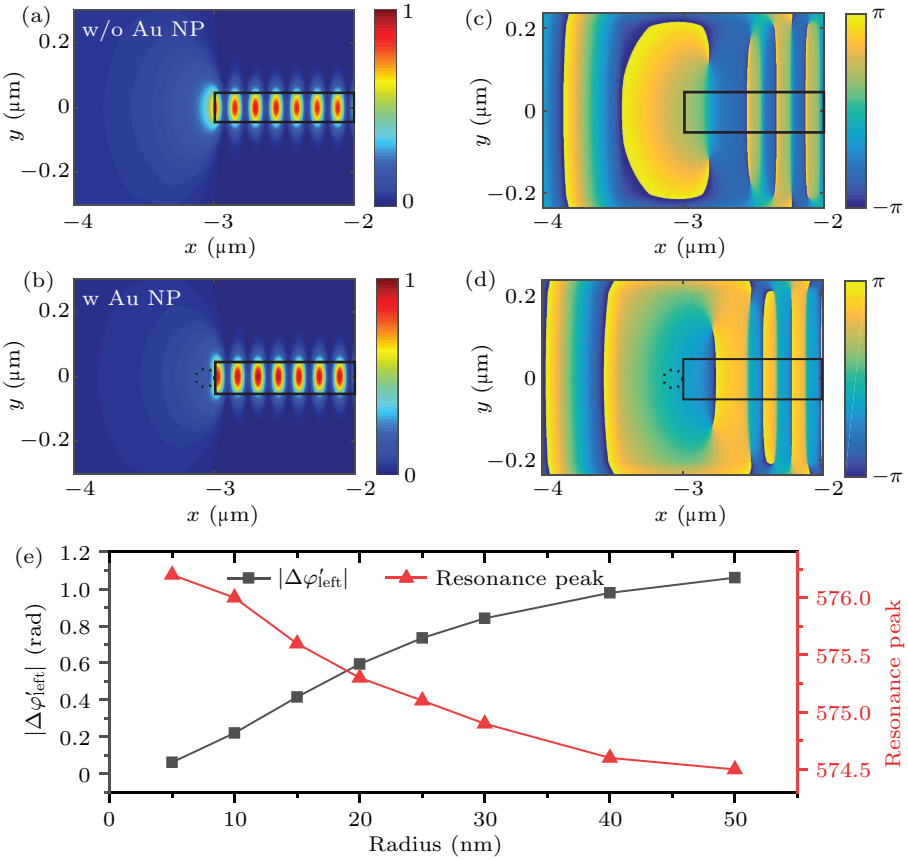


Fig. 4. (a) Local field distribution on the left end facet without Au NP. (b) Local field distribution on the left end facet with Au NP ($R = 25$ nm). (c) Phase diagram of electric field E_z without Au NP. (d) Phase diagram of electric field E_z with Au NP ($R = 25$ nm). Solid black lines represent perovskite nanowire, and black dotted lines represent Au NP. (e) Additional phase difference and resonant peak wavelength at different radii.

A decrease in full width at half maximum (FWHM) of the resonant mode is also found along with the blueshift as shown in Fig. 1, suggesting the promoted quality factor of the nanowire cavity. This point seems not reasonable since the nanoparticle would probably introduce more loss to the microcavity and reduce the quality factor. Figures 5(a) and 5(b) show the normalized transmittance of the end facet as a function of wavelength for nanoparticles of different radii. For nanoparticle radius relatively small, one could observe decreased reflectivity, which would thereby increase the total loss of the microcavity and reduce the quality factor. This point could be easily understood that such small nanoparticle

could bring more scattering losses at the end facet. While the radius of nanoparticles becomes larger, the reflectivity tends to increase and the quality factor becomes better (from 230 to 302) (see Fig. 5(c)), probably due to the increased area of the dielectric–metal interface.

We further investigate the spectral change caused by more than one Au NP. As shown in Fig. 6, the attachment of two Au NPs at the end facets would bring about a blueshift of 2.4 nm, which is exactly twice the blueshift by single Au NP. This indicates that such mechanism for manipulating the cavity resonance could accumulate by increasing the number of interacting nanoparticles.

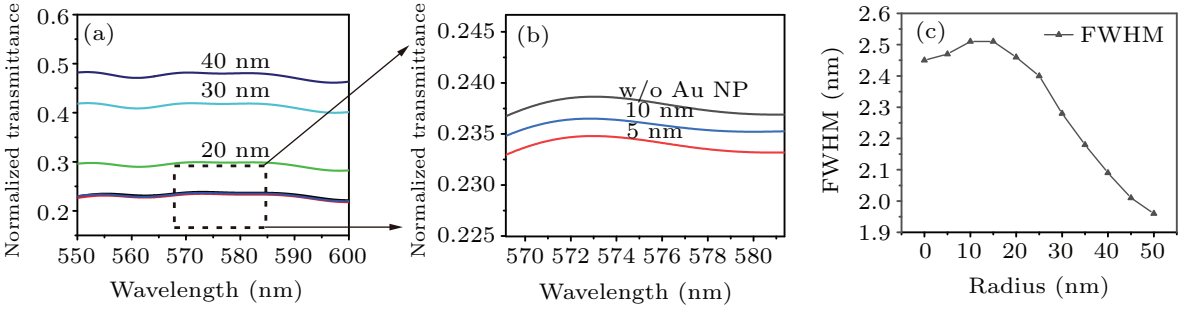


Fig. 5. (a)–(b) The normalized transmittance after reflection only on one side of the end facet for particles with different radii, (b) is a partially enlarged view of (a). (c) The scatter plot of FWHM versus nanoparticle radius.

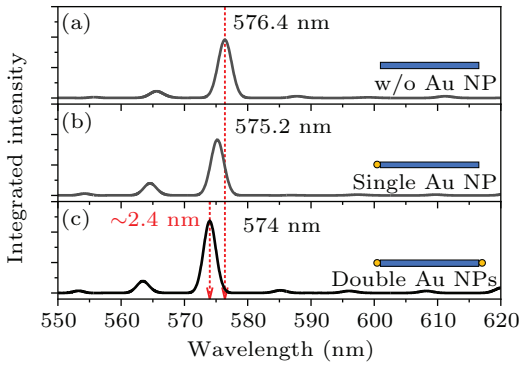


Fig. 6. Simulated spectra (a) without Au NP, (b) with single Au NP, (c) with two Au NPs.

Finally, the ability to control the emission direction is investigated. Initially, laser is mainly emitted from the two end facets of the nanowire. Without attaching the Au NP, there is no difference in emission spectra between the left and right end facets (Fig. 7(a)). After attaching an Au NP (25-nm-radius) at the left facet, unbalanced emission with more laser output from the right facet could be observed (Fig. 7(b)). For increased nanoparticle size (50-nm-radius), such unbalance becomes significantly obvious (Fig. 7(c)), leaving almost no laser exiting from the left side, as seen in Fig. 3(g). Such operation could enable unidirectional emission of nanowire with the help of single Au NP, so as to make the on-chip integration more practical.[22] In addition, we also find that when the attachment position of the gold nanoparticles deviates from the center of the end facet, spatial distribution of output laser would be affected from the end facet. As shown in Figs. 7(d) and 7(e), when a 50-nm-radius nanoparticle is attached to the upper part of the left end facet with an offset of 30 nm from the center, it can be seen that the direction of the emitted laser is obviously tilted. This effect could be further enhanced if high-order mode inside the F-P cavity is taken into consideration.

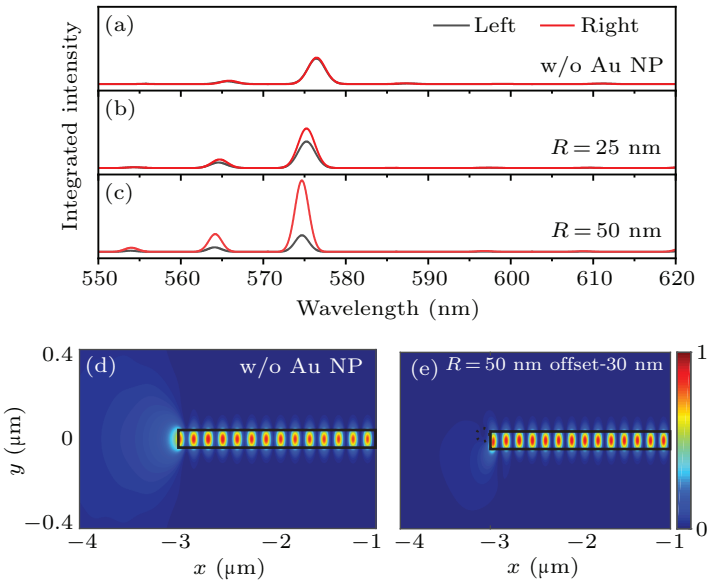


Fig. 7. Comparison of simulated spectra from left and right end facets (a) without Au NPs, (b) with Au NP ($R = 25$ nm), (c) with Au NP ($R = 50$ nm). The local field distribution diagram of perovskite nanowire end-facet emission (d) without Au NP, (e) with Au NP ($R = 50$ nm, 30-nm offset from the center of end facet).

As a supplementary note, we find that the vertical offset of the Au NP at the end facet, would not palpably affect the resonance wavelength, quality factor, and emission direction. This is due to that here our analysis was restricted within the scope of single-mode guiding condition, where only fundamental mode could exist in the nanowire cavity. One may readily expect that, for nanowire cavities with larger widths, high-order traverse modes become available and we could thus manipulate emission direction or select low-order or high-order traverse modes by carefully adjusting the vertical offset of the Au NP at the end facet. Lastly, the feasibility of Au NP manipulations by probes such as fiber tapers[38] makes such mode manipulation experimentally accessible.

4. Conclusion

We have demonstrated a simple method for manipulating cavity modes of F-P type microlasers. The mechanism of introducing or reducing extra optical loss via single Au NPs is theoretically revealed. The influences of the microlaser parameters, including resonant wavelength, quality factor, and emission directions, on the nanoparticle sizes are successively investigated. It is found that blueshift of resonant wavelength could be achieved together with either promoted or degraded quality factor of microlaser via attachment of Au NPs with varied sizes. Unidirectional emission could also be realized via large Au NP, which is favorable for on-chip integration. Considering the feasibility of Au NP manipulations by fiber taper probes, our results provide a useful reference for manipulating microlasers toward the experimental realization of high-performance optoelectronic devices in the future.

Acknowledgements

The authors thank Mr. Y. Lun for helpful discussion.

Project supported by the National Natural Science Foundation of China (Grant Nos. 12174116 and 91850107), the National Key Research and Development Program of China (Grant No. 2018YFA0306200), Guangdong Innovative and Entrepreneurial Research Team Program (Grant No. 2016ZT06C594), and Science and Technology Project of Guangdong (Grant No. 2020B010190001).

References

[1] Ge L, Feng L and Schwefel H G L 2017 *Photonics Res.* **5** OM1
[2] Hill M T and Gather M C 2014 *Nat. Photonics* **8** 908
[3] Ma R M and Oulton R F 2019 *Nat. Nanotechnol.* **14** 12
[4] Miao P, Zhang Z F, Sun J B, Walasik W, Longhi S, Litchinitser N M and Feng L 2016 *Science* **353** 464
[5] Yan J, Wang D N and Li X 2021 *Journal of Lightwave Technology* **39** 5177
[6] Yang S C, Wang Y and Sun H D 2015 *Adv. Opt. Mater.* **3** 1136
[7] Zhang W, Yao J and Zhao Y S 2016 *Acc. Chem. Res.* **49** 1691
[8] Zhang Y, Xie L Z, Li H R, Wang P, Liu S, Peng Y Q and Zhang M 2015 *Chin. Phys. Lett.* **32** 098103
[9] Lee Y H, Jewell J, Scherer A, McCall S, Harbison J and Florez L 1989 *Electron. Lett.* **25** 1377
[10] Ding M, Murugan G S, Brambilla G and Zervas M N 2012 *Appl. Phys. Lett.* **100** 081108
[11] Dong C H, Xiao Y F, Han Z F, Guo G C, Jiang X S, Tong L M, Gu C and Ming H 2008 *IEEE Photon. Technol. Lett.* **20** 342
[12] Dong H Y, Wei Y H, Zhang W, Wei C H, Zhang C H, Yao J N and Zhao Y S 2016 *J. Am. Chem. Soc.* **138** 1118
[13] Eaton S W, Fu A, Wong A B, Ning C Z and Yang P D 2016 *Nat. Rev. Mater.* **1** 16028
[14] Ning C Z 2019 *Adv. Photonics* **1** 014002
[15] Wang K Y, Wang S, Xiao S M and Song Q H 2018 *Adv. Opt. Mater.* **6** 1800278
[16] Wang Y L, Jiang P, Liang K and Yu L 2021 *Appl. Phys. Lett.* **119** 173101
[17] Zhang Q, Su R, Du W N, Liu X F, Zhao L Y, Ha S T and Xiong Q H 2017 *Small Methods* **1** 1700163
[18] Wang K Y, Xing G C, Song Q H and Xiao S M 2021 *Adv. Mater.* **33** 2000306
[19] Fu Y P, Zhu H M, Stoumpos C C, Ding Q, Wang J, Kanatzidis M G, Zhu X Y and Jin S 2016 *ACS Nano* **10** 7963
[20] Couteau C, Larrue A, Wilhelm C and Soci C 2015 *Nanophotonics* **4** 90
[21] Zhu H M, Fu Y P, Meng F, Wu X, Gong Z, Ding Q, Gustafsson M V, Trinh M T, Jin S and Zhu X Y 2015 *Nat. Mater.* **14** 636
[22] Bao Q Y, Li W J, Xu P Z, Zhang M, Dai D X, Wang P, Guo X and Tong L M 2020 *Light Sci. Appl.* **9** 42
[23] Dong H Y, Zhang C H, Lin X Q, Zhou Z H, Yao J N and Zhao Y S 2017 *Nano Lett.* **17** 91
[24] Dong H Y, Zhang C H and Zhao Y S 2019 *Adv. Opt. Mater.* **7** 1900037
[25] Huang C, Sun W Z, Liu S, Li S, Wang S, Wang Y J, Zhang N, Fu H B, Xiao S M and Song Q H 2019 *Laser Photonics Rev.* **13** 1800189
[26] Huang C, Zhang C, Xiao S M, Wang Y H, Fan Y B, Liu Y L, Zhang N, Qu G Y, Ji H G, Han J C, Ge L, Kivshar Y and Song Q H 2020 *Science* **367** 1018
[27] Xiao Y, Meng C, Wang P, Ye Y, Yu H K, Wang S S, Gu F X, Dai L and Tong L M 2011 *Nano Lett.* **11** 1122
[28] Zhang N, Fan Y B, Wang K Y, Gu Z Y, Wang Y H, Ge L, Xiao S M and Song Q H 2019 *Nat. Commun.* **10** 1770
[29] Bergman D J and Stockman M I 2003 *Phys. Rev. Lett.* **90** 027402
[30] Lu Y J, Kim J, Chen H Y, Wu C, Dabidian N, Sanders C E, Wang C Y, Lu M Y, Li B H, Qiu X, Chen L J, Shvets G, Shih C and Gwo S 2012 *Conference on Lasers and Electro-Optics* May 6, 2012 San Jose,California, CTh5C.7
[31] Li C, Liu Z, Chen J, Gao Y, Li M L and Zhang Q 2019 *Nanophotonics* **8** 2091
[32] Ubaid S, Liao F, Guo T, Gu Z Q, Linghu S Y, Ma Y N, Yu J X and Gu F X 2019 *Chin. Opt. Lett.* **17** 121401
[33] Azzam S I, Kildishev A V, Ma R M, Ning C Z, Oulton R, Shalaev V M, Stockman M I, Xu J L and Zhang X 2020 *Light Sci. Appl.* **9** 90
[34] Jin Y Y, Yang L, Pan C X Y, Shi Z X, Cui B W, Xu P Z, Yang Y X, Zhou N, Guo X, Wang P and Tong L M 2021 *Nanophotonics* **10** 2875
[35] Zhou N, Yang Y X, Guo X, Gong J, Shi Z X, Yang Z Y, Wu H, Gao Y X, Yao N, Fang W, Wang P and Tong L M 2022 *Sci. Adv.* **8** eabn2026
[36] Yang A, Hoang T B, Dridi M, Deeb C, Mikkelsen M H, Schatz G C and Odom T W 2015 *Nat. Commun.* **6** 6939
[37] Wang W J, Ramezani M, Vakevainen A I, Torma P, Rivas J G and Odom T W 2018 *Mater. Today* **21** 303
[38] Chen F, Xu C X, Xu Q Y, Zhu Y Z, Wang R, Zhao J, Wang X X, Chen M M and Qin F F 2019 *Opt. Commun.* **452** 400
[39] Wang Y L, Cheng Z Q, Ma L, Peng X N, Hao Z H and Wang Q Q 2015 *Chin. Phys. Lett.* **32** 034205
[40] Lun Y P, Zhan Z Y, Gu F X, Wang P, Yu H K and Li Z Y 2020 *APL Photonics* **5** 061304